

Optical Engineering

SPIEDigitalLibrary.org/oe

Vibration sensor using 2×2 fiber optic coupler

Putha Kishore
Dantala Dinakar
Kamineni Srimannarayana
Pachava Vengal Rao



SPIE

Vibration sensor using 2×2 fiber optic coupler

Putha Kishore
Dantala Dinakar
Kamineni Srimannarayana
Pachava Venkata Rao
National Institute of Technology
Department of Physics
Warangal, Andhra Pradesh 506004, India
E-mail: kishorephd.nitw@gmail.com

Abstract. A simple fiber optic vibration sensor is designed and demonstrated using fiber optic fused 2×2 coupler that utilized the principle of reflected light intensity modulation. In order to avoid source signal power fluctuations and fiber bending losses, the rational output (RO) technique is adopted. A calibrated 1-mm linear and high sensitivity of 0.36 a.u./mm (2.1 mV/ μ m) region of the displacement characteristic curve is considered for vibration measurement. The experimental results show that the sensor is capable of measuring the frequency up to 3500 Hz with $\sim 0.03 - \mu$ m resolution of vibration amplitude over a dynamic range of 0 to 1 mm. The signal-to-noise ratio of the RO is also improved with respect to the sensing signal. In comparison with dual-fiber and bifurcated-bundle fiber, the designed sensor consists only of a single slope that makes the sensor alignment simple by eliminating the dark region and front slope. Simplicity in design, noncontact measurement, high degree of sensitivity, and economical, along with advantages of fiber optic sensors, are the attractive attributes of the designed sensor that lend support to real-time monitoring and embedded applications. © 2013 Society of Photo-Optical Instrumentation Engineers (SPIE) [DOI: [10.1117/1.OE.52.10.107104](https://doi.org/10.1117/1.OE.52.10.107104)]

Subject terms: fiber optic fused 2×2 coupler; displacement; vibration sensor; fast Fourier transform; frequency.

Paper 130752 received May 23, 2013; revised manuscript received Sep. 4, 2013; accepted for publication Sep. 5, 2013; published online Oct. 4, 2013.

1 Introduction

Vibration monitoring has been carried out on important machines, such as power station turbines and generators, to give an early warning of impending conditions which may develop and lead to complete failure and destruction of the components in machines.^{1,2} Continuous monitoring of vibration not only reduces the maintenance and operating costs, but also avoids frequent interruptions of undesirable engine working.³ In general, vibration is measured by electromechanical devices such as piezoelectric, piezoresistive, or capacitive accelerometers. These types of measurements require physical contact with the vibrating object. However, some noncontact vibration measurement techniques have been developed with optical interferometry and fiber optics. Especially, such noncontact sensors made with optical fibers have already established and played a key role in sensing several physical parameters like vibration, displacement, and pressure.⁴ So, the fiber optic sensors are replacing the conventional sensors due to their distinguished advantages like immunity to electromagnetic interference (EMI), small size, flexible length of the fiber, remutable, high accuracy, secure data transmission, potentially easy to install, and noncorrosive.⁵⁻⁸ Reported fiber optic vibration sensors are in general divided into two types according to their working principle: phase or intensity modulation. The phase-modulated fiber optic interferometric techniques such as Fabry-Perot,⁹ Michelson or Mach-Zehnder,¹⁰ self-mixing,¹¹ and Doppler vibrometry^{12,13} were deployed for vibration measurements. These sensors are more accurate than intensity-modulated sensors and can be used over a large dynamic range. However, they are

often highly expensive, suffer from low degree of stability, and require critical alignment. Consequently, these sensors are not suitable for industrial applications.¹⁴ However the second one i.e. intensity modulated technique takes the advantage by providing change in intensity corresponds to vibration by using simple fiber optic geometry.¹⁵

In this article, we report a simple noncontact intensity-modulated fiber optic vibration sensor design with fiber optic fused 2×2 coupler.¹⁶ It consists of four ports, the first for the coupling of light source, the second to act as a sensing probe, the third is connected to the sensing photodetector, and the fourth is connected to another photodetector, which act as a reference. Here, the single fiber alone is used to guide the light to incident on the reflected surface glued on the sensing part of the vibrating object and to receive the reflected light. In comparison to dual-fiber and bifurcated bundle fiber, which exhibit two slopes, the designed sensor consists of only a single slope that makes the sensor alignment simple by eliminating the dark region and front slope.^{17,18} Moreover, the rational output (RO) between the sensing and the reference signals minimizes the effect of source fluctuations and bending losses at the source end.¹⁹

2 Theory and Design of the Sensor

In general, the required major quantity to measure the vibration is displacement. The velocity and acceleration can be measured from the displacement, because these parameters are inter-related to each other.²⁰ The noncontact fiber optic vibration sensor is working based on the reflected light intensity modulation with respect to the displacement between the sensing fiber probe and the reflecting surface. The basic principle of vibration measurement is intensity modulation, due to the displacement of the reflecting surface glued to the

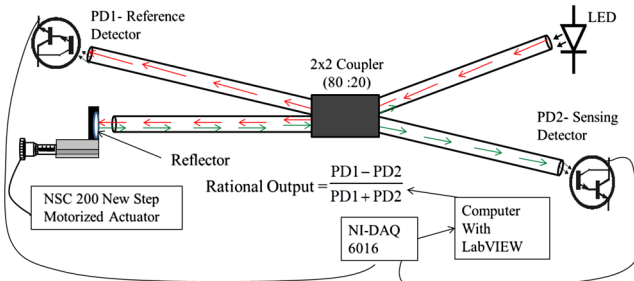


Fig. 1 Schematic of the experimental setup for the displacement response of the sensor.

vibrating target from the sensing fiber probe. The light guiding mechanism through the coupler is shown in Fig. 1. A light source of power P_a is coupled to port A of the coupler and is directed to port B. The light incident onto the reflector via port B is reflected back into the same fiber (port B) and is a function of the gap “ x ” between the sensing fiber probe (port B) and the reflector. The light is transmitted from the source with a power P_a through the port A to the sensing fiber (port B), and then incident on the reflector, which is given by²¹

$$P_b = (1 - cr)(10^{-0.1L} - 10^{-0.1D})P_a, \quad (1)$$

where cr , L , and D are coupling ratio, excess loss, and directivity of the fiber coupler, respectively. The cross section of the sensing fiber is positioned parallel to the reflecting surface, and the reflected light of power P_c coupled back into the same fiber (port B), which is given by

$$P_c = P_i \left[1 - \exp \left(-\frac{2a^2}{W^2(x)} \right) \right], \quad (2)$$

where $P_i = kP_b$ is the light power coupled to the sensing fiber at $x = 0$, a is the core radius of the fiber, $W(x) = 2x \tan(\theta) + a$, $k = 1.15$, and $\theta = \sin^{-1} NA$ is the divergence angle of the fiber. Substituting Eq. (1) into Eq. (2) and written as

$$P_c = k(1 - cr)(10^{-0.1L} - 10^{-0.1D})P_a \left[1 - \exp \left(-\frac{2a^2}{W^2(x)} \right) \right]. \quad (3)$$

The light power detected by the photodetector from the sensing port through the port C is given by

$$P_d = kcr(10^{-0.1L} - 10^{-0.1D})P_c. \quad (4)$$

Substituting $W(x)$, Eq. (3) into Eq. (4) yields

$$P_d = cr(1 - cr)(10^{-0.1L} - 10^{-0.1D})^2 \times \left[1 - \exp \left(-\frac{2}{(2x \tan(\theta) + a)^2} \right) \right] P_a. \quad (5)$$

Therefore

$$P_d = P \left[1 - \exp \left(-\frac{2}{(2x \tan(\theta) + a)^2} \right) \right] P_a, \quad (6)$$

where $P = 1.15cr(1 - cr)(10^{-0.1L} - 10^{-0.1D})^2$.

For a large value of $2x \tan \theta / a$, Eq. (6) can be written as

$$P_d = \frac{P}{2} \left[\frac{(2a)^2}{[2x \tan(\theta)]^2} \right] P_a. \quad (7)$$

Therefore, the power received by the photodetector at sensing end is directly proportional to the square of the fiber diameter and inversely proportional to the square of the distance between the sensing fiber probe and the reflector.²²

Figure 1 illustrates a plastic multimode fiber optic 2×2 fused coupler (IF-541) made of polymethyl methacrylate having a split ratio of 80:20, which is used as a vibration sensor. It has low attenuation in the visible region and can be operated in the temperature range from -55°C to 70°C . An light emitting diode (LED) (IF-E96) of peak wavelength 650 nm having a typical fiber launching power of $200 \mu\text{W}$ is used as a source, and two numbers of photodarlington detector (PD) of high sensitivity housed in a connector less package (IF-D93) are used to detect the intensity of light at the reference and sensing ends. A simple detection circuit is designed to convert the modulated light intensity into its equivalent voltage signal, and an NI-DAQ 6016 with LabVIEW software is used to record the time-domain signal (TDS) of the reference and the sensing signals from which the RO is calculated.

The fiber optic fused 2×2 coupler has core/cladding diameters of $980/1000 \mu\text{m}$ and measures 100-cm length with a splitting ratio of 80:20. All four ports of the coupler are used for the vibration detection. The LED light coupled to port A split in to the ratio of 80:20, part of light (80%) is transmitted through port B, which acts as a sensing probe, and the other part (20%) is directed toward PD1 through port D, which is used as a reference. The light passed through port B projects onto a weightless plastic reflector having reflectivity of 40% which is attached to the center of the speaker diaphragm (vibrating object). The modulated reflected light corresponding to vibration is recoupled into the same fiber (port B) and is directed to PD2 through port C. In addition, to avoid the effect of source signal power fluctuations and fiber bending losses, the RO of PD1 and PD2 is measured and can be expressed as

$$\text{Rational Ouput(RO)} = \frac{PD1 - PD2}{PD1 + PD2}. \quad (8)$$

A suitable calibration has been taken from the experimental displacement characteristic curve of the sensor, as shown in Fig. 2, which follows the inverse square law as given by Eq. (7), and the linear part of the curve is used for the vibration measurement. New Step Motorized Actuator NSC200 along with NSA12 micrometer replacement actuator operated with NewStep-Util software 303A are used to move the reflector attached to the micrometer stage to and from the sensing probe with a step size of $1 \mu\text{m}$ over a dynamic range of 4 mm. The data curve representing the

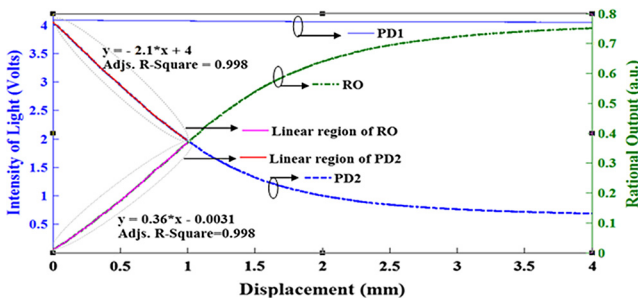


Fig. 2 Characteristic displacement curve of the sensor.

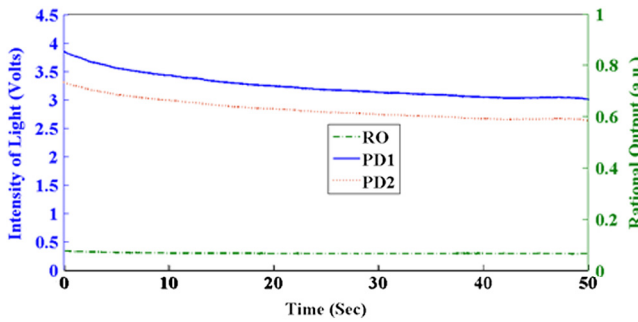


Fig. 3 Effect of source fluctuation on PD1, PD2, and rational output (RO).

response of PD2 with respect to the displacement of the reflector from the sensing probe (Fig. 2) has a linear region of about 1 mm with high sensitivity of $2.1 \text{ mV}/\mu\text{m}$, whereas the data curve representing the RO has the sensitivity of $0.36 \text{ a.u.}/\text{mm}$, which is considered for vibration measurement.

Before going to vibration measurement, the sensor response is tested for both source fluctuation and fiber bending at the source end. Figure 3 shows the effect of source fluctuation on the sensing and the reference signals. The measured signals from PD1 and PD2 show a change in intensity of light with respect to variation in light intensity of LED by means of varying driving voltage, whereas the RO of these signals shows insensitivity to source fluctuations. It can be observed from the test results that the RO method enables minimization of the effect of source fluctuation on the sensor response. To study the fiber bending losses on the sensor output, the fiber is bended by using a microbending pressure element. Figure 4 illustrates the effect of fiber microbending at the source end (port A) on individual outputs of PD1 and PD2 as well as on RO of both the signals. It is evident from the test results that there is no effect on RO, whereas outputs of PD1 and PD2 are affected by the fiber bending.

3 Experimental Setup

The schematic experimental setup of the vibration sensor is shown in Fig. 5. The whole setup is mounted on a vibration-free table (Newport, Franklin). To test the sensor response for corresponding vibrations, a synthesized function generator (HM8130, Scientific) and a commercial speaker having dimensions of 25-mm depth and 65-mm diaphragm along the diagonal with a calibrated reflector attached at the center

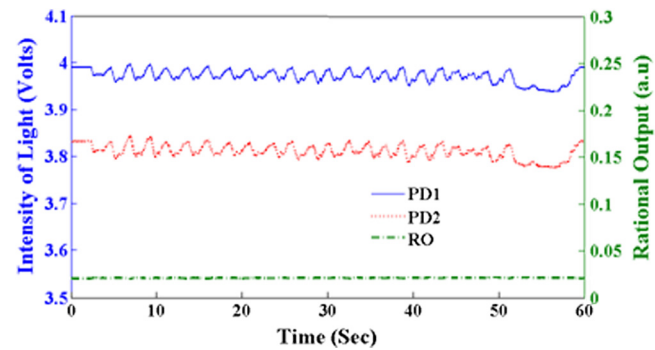


Fig. 4 Effect of bending on the output of PD1, PD2, and RO.

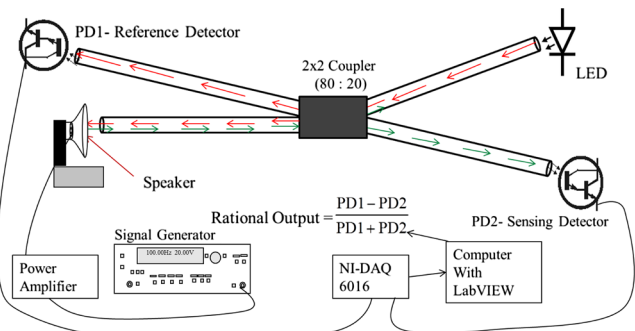
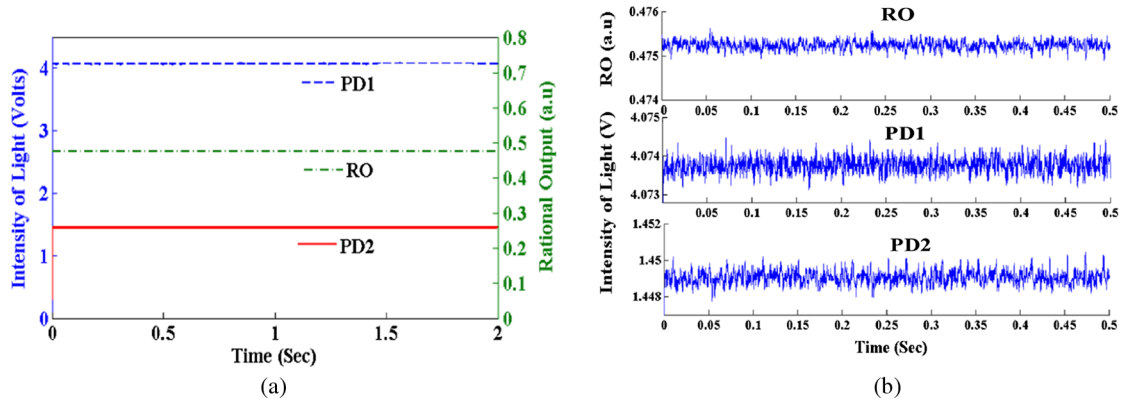
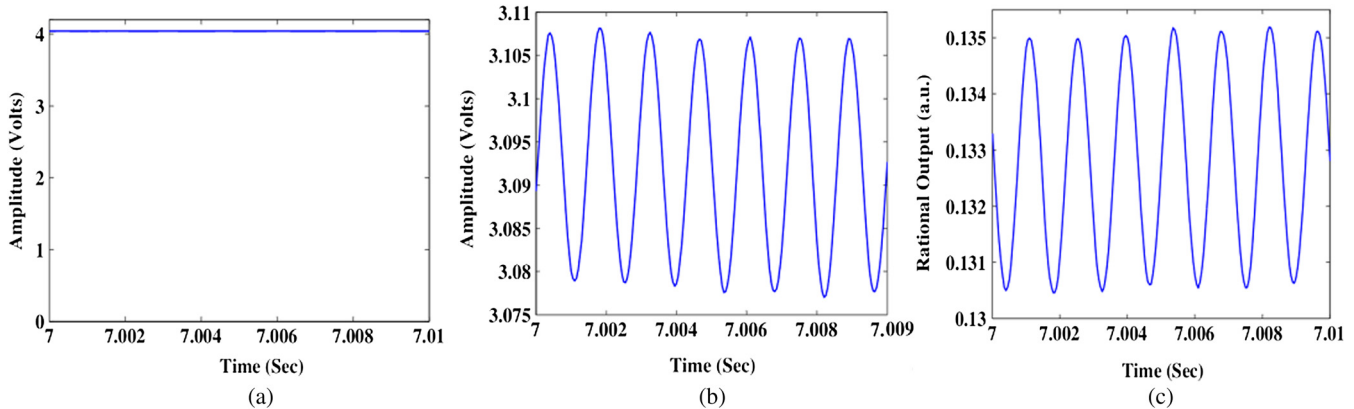


Fig. 5 Schematic experimental setup for vibration measurement.

of the dust cap (diaphragm) are used. A data acquisition (DAQ) system is used to record the TDS of the sensor and to monitor the vibrations of the speaker at different known frequencies and amplitudes (driving voltages). Most of the vibrations are sinusoidal displacement of the vibrating object about its mean position. Generally, vibrations of this nature can be measured by their amplitude and frequency. So, the fast Fourier transform (FFT) technique is used to convert the TDS response into frequency domain response to analyze the vibration in terms of frequency of the vibrating object and also to measure the amplitude of vibration. The experiment is repeated for different frequencies of amplitude of vibration to measure the detectable maximum frequency, amplitude resolution, and to test the reliability of the sensor.

4 Results and Discussion

Figure 6(a) shows the signals of PD1 and PD2 and RO of these signals at constant distance of the sensing probe from the diaphragm center of the speaker. This reveals the stability of the detection signals. The signal-to-noise ratio (SNR) calculated for the normalized RO, PD1, and PD2 signals are found to be 77.55, 92.54, and 74.70 dB, respectively. It is evident that the SNR of the RO is improved when compared with PD2, as shown in Fig. 6(b). The sine wave is applied to the speaker, and corresponding TDS response of the sensor is recorded by using NI-DAQ at the frequency of 700 Hz, as shown in Fig. 7. The FFT of the TDS signal gives the frequency of the signal and observed a perfect matching between the frequencies of applied and sensing signals. The peak-to-peak voltage of the output signal gives the amplitude of vibration using the slope of the calibration curve, which corresponds to displacement amplitude

**Fig. 6** (a) Stability of the signals and (b) noise of the signals.**Fig. 7** The waveforms of time-domain signal (TDS) at 700 Hz (a) PD1, (b) PD2, and (c) RO.

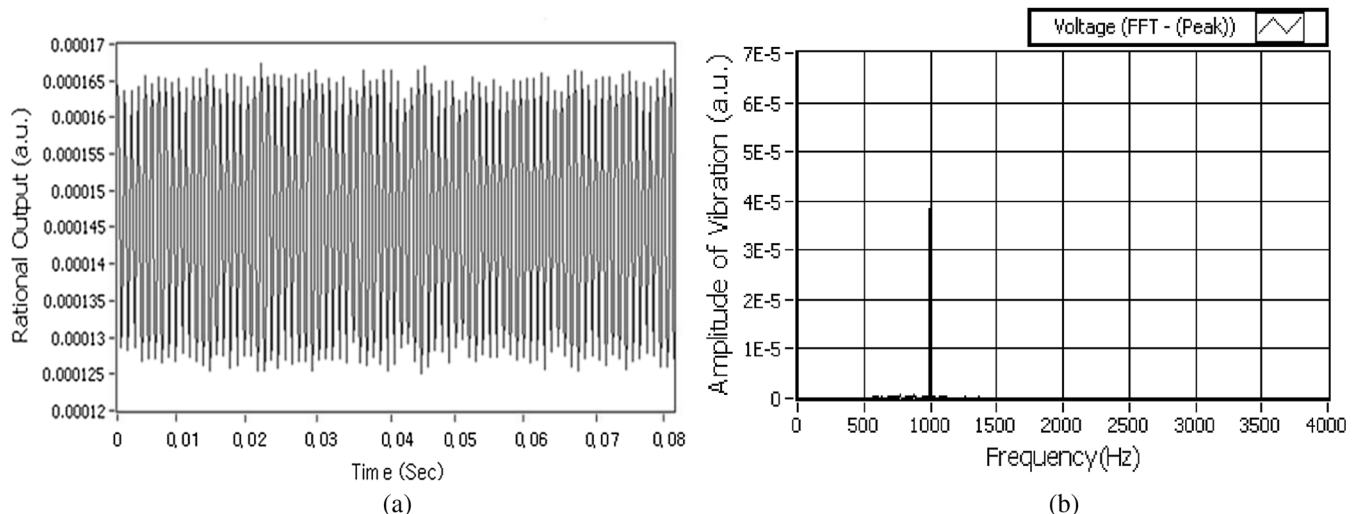
d_p . For a given frequency f_p , the peak velocity v_p and the peak acceleration a_p can be computed by²⁰

$$a_p = (2\pi)^2 f_p^2 d_p. \quad (10)$$

$$v_p = (2\pi)f_p d_p, \quad (9)$$

and

The sensed TDS waveform which is recorded by the DAQ and by the corresponding FFT spectrum at 1-kHz signal applied to the speaker is shown in Fig. 8. Figure 9 illustrates the relation between the frequency applied to the speaker and the frequency measured by the sensor. At constant amplitude

**Fig. 8** (a) TDS waveform of RO of the PD1 and PD2 signals and (b) spectrum of FFT of the corresponding RO signal at 1 kHz.

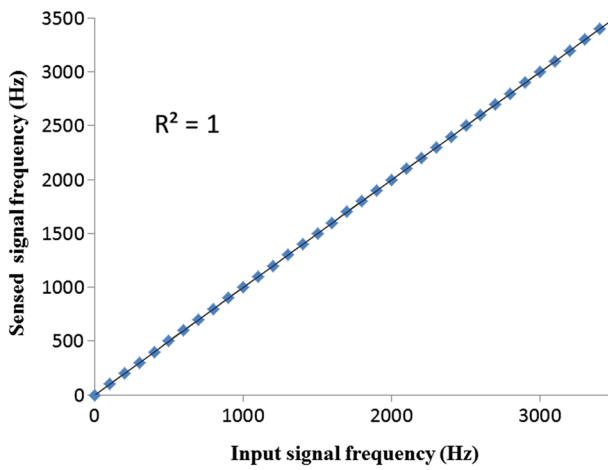


Fig. 9 Frequency response of the vibration sensor.

of vibration, i.e., at constant driving voltage, the range of frequency 0 to 3500 Hz is applied to the speaker, and the corresponding frequency measured by the sensor is recorded. The obtained results show that up to 3500 Hz, there is a perfect matching between the frequency applied to the speaker and that measured by the sensor output. In between 3500 to 4000 Hz, the sensor exhibits an error of ± 5 Hz may be attributed to the fact that the noise in the sensing signal is dominating, and beyond 4000 Hz, there is no response from the sensor and exhibits only DC signal. The frequency bandwidth depends only on the detection system that are photo-detector response, sampling rate of the DAQ, and efficiency of electronic circuitry, but not on the fiber properties.

The sensor is also tested for the amplitude response as shown in Fig. 10 at the constant frequency 390 Hz. It is evident from Fig. 10 that the amplitude of the signal applied to the speaker is constant for a period of 1.1 s; further, the damped decay of the signal represents that the signal generator is switched off followed by the DC signal up to 1.25 s, and this indicates the stability of the signal. After that, the damped vibration following the DC signal corresponds to the state of the signal generator being switched on and off within a small period of time. Figure 11 depicts the sensor output at a constant frequency of 100 Hz for varying amplitude of vibration. The amplitude response of the sensor between driving voltage applied to the speaker and FFT peak voltage of the output signal at different frequencies

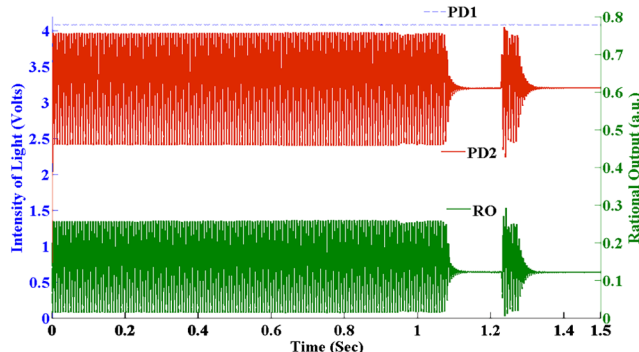


Fig. 10 The amplitude response of the sensor for the corresponding speaker vibration at 390 Hz.

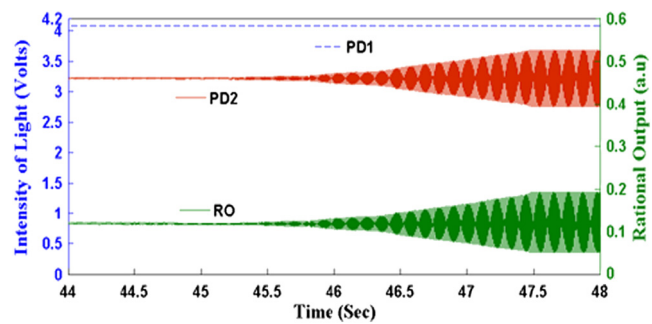


Fig. 11 TDS spectra of the sensor correspond to continuous variation in amplitude at 100 Hz.

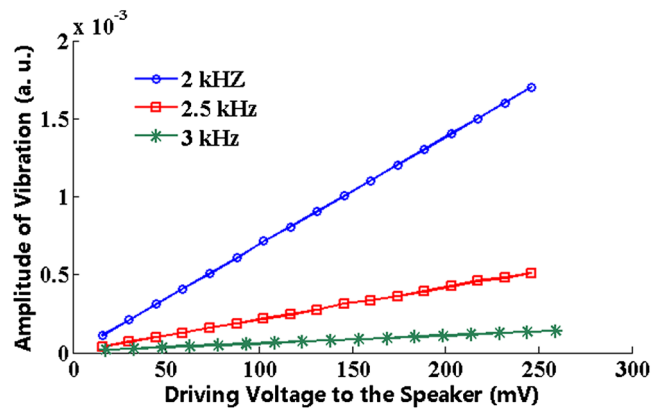


Fig. 12 Amplitude response of the sensor at different frequencies.

is plotted in Fig. 12. It is observed that the amplitude of vibration is linear with the correlation coefficient of about 0.99 in response to the driving voltage applied to the speaker. The change in amplitude sensitivity with respect to the change in frequency is plotted in Fig. 13. It represents the speaker amplitude response at different frequencies, and the subplot shows the resonance frequency of the speaker of about 2 kHz. The resolution of the sensor is calculated from the minimum amplitude of vibration detected by the sensor at maximum frequency. The sensitivity of the vibration sensor is found to be 0.36 a.u./mm (2.1 mV/ μ m) over a

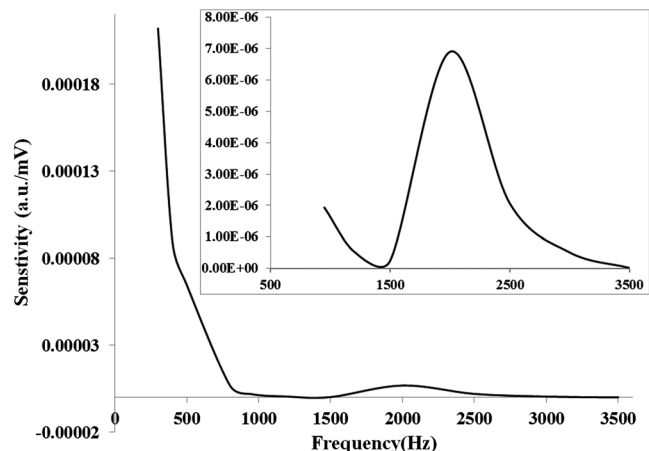


Fig. 13 The variation of the amplitude sensitivity with respect to the frequency.

span of 0 to 1-mm linear slope of the displacement characteristic curve. Experimentally, the minimum amplitude resolvable by the sensor is $1\text{E} - 5$ a.u., which corresponds to the resolution of $0.028\text{ }\mu\text{m}$. The experiment is repeated to test the reliability, and the response of the sensor system is found to be consistent.

In general, the possibilities of error that might occur in noncontact intensity-modulated measurements are fluctuation in the source light, the light stray effect, and dust formation on the mirrors. A hollow cylindrical protection tool is arranged surrounding the reflector, which restricts interference of the stray light with the source light and too avoids the formation of dirt on the mirror. As the sensor is positioned very close to that of the vibrating target within the linear region of the sensor, it benefits from no requirement of special optics, which is especially useful for sensing applications in embedded situations.

5 Conclusions

In this article, a simple geometrical intensity-modulated noncontact vibration sensor has been presented using a 2×2 fiber optic-fused coupler. A single fiber is used as sensing probe, which results in single slope with high sensitivity of 0.36 a.u./mm ($2.1\text{ mV}/\mu\text{m}$) over a dynamic range of 1-mm linear region, facilitating easy alignment and accurate measurement. Minimized effects of source signal fluctuations and fiber bending losses on sensing is noted by adopting the RO technique. The experimental results show that the sensor is able to measure the frequency up to 3500 Hz with $\sim 0.03 - \mu\text{m}$ resolution of vibration amplitude over a span of 0 to 1 mm. It is also observed that the SNR of RO is improved with respect to the sensing signal. In comparison with dual-fiber and bifurcated-bundle fiber, this sensor adds the advantage of eliminating the dark region and front slope, which facilitates easy alignment. Simple in design, noncontact measurement, high degree of sensitivity, and economical, along with advantages of fiber optic sensors, are the attractive attributes of the sensor that lend support to real-time monitoring and embedded applications.

References

1. J. D. Zook et al., "Fiber optic vibration sensor based on frequency modulation of light-excited oscillators," *Sens. Actuators* **83**(1–3), 270–227 (2000).
2. J. Slavic et al., "Measurement of the bending vibration frequencies of a rotating turbo wheel using an optical fiber reflective sensor," *Meas. Sci. Technol.* **13**(4), 477–482 (2002).
3. B. G. Liptac, *Instrument Engineer's Handbook: Process Measurement and Analysis*, 4th ed., Vol. 1, pp. 1102–1117, CRC Press, Boca Raton (2003).
4. D. A. Krohn, *Fiber Optic Sensors: Fundamentals and Applications*, 2nd ed., Instrument Society of America, North Carolina (1992).
5. C. Brain and J. Dakin, *Optical Fiber Sensors: Applications, Analysis, and Future Trends*, Vol. 4, Artech House Inc., Boston (1997).
6. Y. Alayli et al., "Applications of a high accuracy optical fiber displacement sensor to vibrometry and profilometry," *Sens. Actuators A* **116**(1), 85–90 (2004).
7. M. L. Casalicchio, G. Perrone, and A. Valla, "A fiber optic sensor for displacement and acceleration measurements in vibration tests," in *IMTC2009*, pp. 5–7, IEEE, Singapore (2009).
8. M. R. Saad, M. Rehman, and O. Siddiqui, "Development of linear fiber optic pressure sensor," in *IEEE LTIMC2004*, IEEE, Palisades, New York (2004).
9. N. Sathitanon and S. Pullteap, "A fiber optic interferometric sensor for dynamic measurement," *World Acad. Sci. Eng. Technol.* (11), 246–249 (2007).
10. S. Donati, *Electro-Optical Instrumentation: Sensing and Measuring with Lasers*, Prentice Hall, Upper Saddle River (2004).

11. G. Giuliani et al., "Laser diode self-mixing technique for sensing applications," *J. Opt. A Pure Appl. Opt.* **4**(6), S283–S294 (2002).
12. P. Castellini, M. Martarelli, and E. P. Tomasini, "Laser Doppler vibrometry: development of advanced solutions answering to technology's needs," *Mech. Syst. Signal Process.* **20**(6), 1265–1285 (2006).
13. A. Chijoike and J. Lawall, "Laser Doppler vibrometer employing active frequency feedback," *Appl. Opt.* **47**(27), 4952–4958 (2008).
14. J. Chang et al., "Fiber Bragg grating acceleration sensor interrogated by a DFB laser diode," *Laser Phys.* **19**(1), 134–137 (2009).
15. S. Binu et al., "PMMA (polymethyl methacrylate) fiber optic probe as a noncontact liquid level sensor," *Microwave Opt. Technol. Lett.* **52**(9), 2114–2118 (2010).
16. V. K. Kurkarni et al., "Fiber optic micro-displacement sensor using coupler," *J. Optoelectron. Adv. Mater.* **8**(4), 1610–1612 (2006).
17. P. Kishore et al., "Fiber optic vibration sensor using PMMA fiber for real time monitoring," *Sens. Transducers J.* **136**(1), 50–58 (2012).
18. P. Kishore et al., "Non-contact vibration sensor using bifurcated bundle fiber for real time monitoring of diesel engine," *Int. J. Optoelectron. Eng.* **2**(1), 4–9 (2012).
19. J. Chang et al., "Fiber optic vibration sensor based on over-coupled fused coupler," *Proc. SPIE* **6595**, 65954C (2007).
20. G. C. King, *Vibrations and Waves*, pp. 5–10, John Wiley & Sons Ltd., West Sussex, United Kingdom (2009).
21. Y. Samian et al., "Theoretical and experimental study of fiber-optic displacement sensor using multimode fiber coupler," *J. Optoelectron. Biomed. Mater.* **1**(3), 303–308 (2009).
22. M. Yasin et al., "Simple design of optical fiber displacement sensor using a multimode fiber coupler," *Laser Phys.* **19**(7), 1446–1449 (2009).



Putha Kishore received his BSc and MSc degrees specializing in electronics and communications at Sri Venkateswara University, Tirupati, Andhra Pradesh, in 2006 and 2008, respectively. He is currently pursuing a PhD degree, while investigating fiber optics for vibration measurement at the Department of Physics, NIT Warangal, Andhra Pradesh. His research interests include optical fiber vibration sensors, fiber Bragg grating sensors, and specialty fiber optic sensors. He has published 12 articles in journals and 18 articles in conferences. He is a member of SPIE and OSA.



Dantala Dinakar received his BSc degree from Kakatiya University, Warangal, Andhra Pradesh, in 1980, MSc (Tech.) degree specializing in applied electronics from Osmania University, Hyderabad, Andhra Pradesh, in 1983, and PhD degree in microwave communications from National Institute of Technology, Warangal, Andhra Pradesh, in 1992. He has been a faculty member of the Department of Physics at National Institute of Technology, Warangal, Andhra Pradesh, since 1991. His research interests are in the areas of microwave communications, fiber-optic sensors, passive components in telecommunications, and optical techniques in precision measurements. He has authored over 15 technical publications. He is a member of SPIE.



Kamineni Srimannarayana received his BSc degree from Andhra University, Visakhapatnam, Andhra Pradesh, in 1971, and MSc (Tech.) and PhD degrees in engineering physics in the fields of photonics and holography for NDT from National Institute of Technology (Deemed University), Warangal, Andhra Pradesh, in 1974 and 1978, respectively. He has been a faculty member of the Department of Physics at National Institute of Technology, Warangal, Andhra Pradesh, since 1977. His research interests are in the areas of fiber-optic sensors, passive components in telecommunications, optical techniques in precision measurements, laser metrology, and holography for NDT. He has authored over 90 technical publications. He is a member of SPIE and OSA.



Pachava Vengal Rao received his BSc and MSc degrees specializing in electronics and communications from Osmania University, Hyderabad, Andhra Pradesh, in 2004 and 2009, respectively. He is currently pursuing a PhD degree, while investigating the use of optical sensing techniques at the Department of Physics, NIT Warangal, Andhra Pradesh. His research interests include low- and high-pressure sensing using fiber Bragg grating sensors. He has published 8 articles in international journals and 14 articles in international conferences. He is a fellow of Optical Society of India, member of SPIE, and OSA.